

An exact nonlinear hybrid-coordinate formulation for flexible multibody systems

Jinyang Liu · Jiazhen Hong · Lin Cui

Received: 28 March 2007 / Accepted: 17 September 2007 / Published online: 8 November 2007
© Springer-Verlag 2007

Abstract The previous low-order approximate nonlinear formulations succeeded in capturing the stiffening terms, but failed in simulation of mechanical systems with large deformation due to the neglect of the high-order deformation terms. In this paper, a new hybrid-coordinate formulation is proposed, which is suitable for flexible multibody systems with large deformation. On the basis of exact strain–displacement relation, equations of motion for flexible multibody system are derived by using virtual work principle. A matrix separation method is put forward to improve the efficiency of the calculation. Agreement of the present results with those obtained by absolute nodal coordinate formulation (ANCF) verifies the correctness of the proposed formulation. Furthermore, the present results are compared with those obtained by use of the linear model and the low-order approximate nonlinear model to show the suitability of the proposed models.

Keywords Nonlinear hybrid-coordinate formulation · Flexible multibody systems · Large deformation

1 Introduction

In the linear hybrid coordinate formulation for flexible multibody systems, the quadratic deformation terms are not included in the strain–displacement relation. Therefore, such

formulation fails to explain the stiffening phenomenon during the simulation of a rotating flexible beam with high rotating speed [1]. In the recent 10 years, several formulations for investigation of stiffening problems were proposed. Wallrapp [2] and Ryu [3] developed the system equations of motion of flexible multibody systems that include stress stiffening effects. The stress stiffness matrix was derived from the internal virtual work that includes nonlinear terms of strain–displacement relationship and reference stresses induced by existing loads before deformation. Liu [4] investigated the dynamic stiffening problem of a rotating beam with high rotating speed. By using an axial stretch variable, elastic strain was linearized, such that computational efficiency can be improved, and a criterion on inclusion of stiffening terms of a beam was put forward by using an influence ratio [5], and then an experiment was carried out to verify the correctness of the nonlinear formulation [6]. Due to the inclusion of the quadratic deformation terms in the strain–displacement relationship, these formulations succeeded in capturing the stiffening terms in the equations of motion. However, with the assumption of small deformation, the high-order deformation terms in the mass and force matrices were neglected. Because only the low-order deformation terms are taken into account, these formulations are called the low-order approximate formulation, which is not suitable for the dynamic analysis of flexible multibody systems with large deformation.

The absolute coordinate formulation has been widely used for the dynamic analysis of a flexible beam system with large deformation in the recent 10 years [7–9]. In such formulation, the absolute coordinates and slopes defined in global frame are used to describe the element configuration, and an exact strain–displacement relationship is employed, so that geometric nonlinear terms are naturally taken into account. Furthermore, the mass and force matrices are constant, therefore, approximation of the mass and force matrices are not

The project supported by the National Natural Science Foundation of China (10472066, 50475021).

J. Liu (✉) · J. Hong · L. Cui
Department of Engineering Mechanics,
Shanghai Jiaotong University,
Shanghai 200030, China
e-mail: liujy@sjtu.edu.cn

necessary in the absolute coordinate formulation. Recently, this formulation has been extended to spatial beams [10], plates [11], and flexible multibody systems [12]. However, by using absolute coordinates, the variables, which describe the rigid-body motion and deformation, cannot be directly obtained by solving the differential equations because they are not included in the generalized coordinates.

In order to increase the computational accuracy and avoid the simulation error due to the neglect of high-order deformation terms, a new hybrid-coordinate formulation is proposed combining the characteristics of both the hybrid-coordinate formulation and the ANCF. By employing the relative coordinates and slopes defined in the body-fixed frame instead of the deformation coordinates, the mass and force matrices are simplified without the need to consider high-order deformation terms. On the basis of exact strain–displacement relation, such formulation is suitable for flexible multibody systems with large deformation. By using the virtual work principle, the equations of motion for a flexible body are derived, and then Lagrange’s equations of the first kind with Lagrange multipliers are assembled. In addition, a matrix separation method is put forward to improve the efficiency of the calculation. Agreement of the present results with those obtained by the ANCF verifies the correctness of the present formulation. Finally, the results obtained by the proposed formulation are compared with those obtained by use of the previous low-order approximate nonlinear formulations to show the wide suitability of the proposed formulation.

2 Description of kinematics

A flexible multibody system is composed of N bodies: B_i , ($i = 1, \dots, N$). As shown in Fig. 1, e_0 is the inertial frame, and e_i is the body-fixed frame of B_i . The absolute displacement vector of an arbitrary point of the flexible body B_i is given by

$$r = r_0 + s, \tag{1}$$

where r_0 represents the displacement vector of the origin of e_i , and s is the displacement vector of the point with respect to e_i after deformation, we rewrite Eq. (1) as

$$r = r_0 + As', \tag{2}$$

where s' represents s defined in e_i , and A represents the transformation matrix. By using the finite element method, s' can be written as

$$s' = Np, \tag{3}$$

where N is the shape matrix, and p is the elastic coordinate vector.

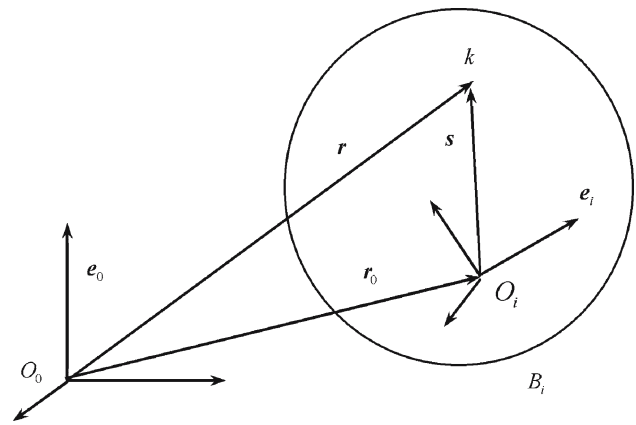


Fig. 1 A flexible body undergoes large overall motion

Differentiating Eq. (2) leads to

$$\dot{r} = \dot{r}_0 - A\tilde{s}'\dot{\omega}' + A\dot{s}' = \dot{r}_0 - A\tilde{s}'\dot{\omega}' + AN\dot{p}, \tag{4}$$

and differentiating Eq. (3) leads to

$$\ddot{r} = \ddot{r}_0 - A\tilde{s}'\ddot{\omega}' + AN\ddot{p} + A\tilde{\omega}'\dot{\omega}'s' + 2A\tilde{\omega}'N\dot{p}, \tag{5}$$

where ω' and $\dot{\omega}'$ represent the angular velocity and angular acceleration defined in the body-fixed frame, respectively, and \tilde{s}' represents the skew-symmetric matrix corresponding to s' .

3 Variational equations of a flexible body

3.1 Virtual work of the inertia force

The virtual displacement coordinate vector reads

$$\delta r = \delta r_0 - A\tilde{s}'\delta\pi' + AN\delta p, \tag{6}$$

where $\delta\pi'$ represents the variation of the rotational displacement vector defined in the body-fixed frame, and then the virtual work of the inertia force can be written as

$$\delta W_i = - \int_V \rho \delta r^T \ddot{r} dV, \tag{7}$$

where ρ represents the mass density of the flexible body.

Substitute Eqs. (5) and (6) into Eq. (7), virtual work of the inertia force is given by

$$\delta W_i = \delta q^T (-M\ddot{q} + Q_i), \tag{8}$$

where $q = [r_0^T \pi'^T p^T]^T$ represents the generalized coordinate vector, and the generalized mass and inertia force

matrices take the form

$$\begin{aligned}
 \mathbf{M} &= \begin{bmatrix} \mathbf{M}_{11} & \mathbf{M}_{12} & \mathbf{M}_{13} \\ \mathbf{M}_{21} & \mathbf{M}_{22} & \mathbf{M}_{23} \\ \mathbf{M}_{31} & \mathbf{M}_{32} & \mathbf{M}_{33} \end{bmatrix}, \\
 \mathbf{Q}_i &= \begin{bmatrix} \mathbf{Q}_1 \\ \mathbf{Q}_2 \\ \mathbf{Q}_3 \end{bmatrix},
 \end{aligned}
 \tag{9}$$

where

$$\begin{aligned}
 \mathbf{M}_{11} &= \rho V \mathbf{I}, \\
 \mathbf{M}_{12} &= \mathbf{M}_{21}^T = - \int_V \rho \mathbf{A} \tilde{\mathbf{s}}' dV,
 \end{aligned}
 \tag{10}$$

$$\begin{aligned}
 \mathbf{M}_{13} &= \mathbf{M}_{31}^T = \int_V \rho \mathbf{A} \mathbf{N} dV, \\
 \mathbf{M}_{22} &= \int_V \rho \tilde{\mathbf{s}}'^T \tilde{\mathbf{s}}' dV = - \int_V \rho \tilde{\mathbf{s}}' \tilde{\mathbf{s}}' dV,
 \end{aligned}
 \tag{11}$$

$$\mathbf{M}_{23} = \mathbf{M}_{32}^T = - \int_V \rho \tilde{\mathbf{s}}'^T \mathbf{N} dV = \int_V \rho \tilde{\mathbf{s}}' \mathbf{N} dV,
 \tag{12}$$

$$\mathbf{M}_{33} = \int_V \rho \mathbf{N}^T \mathbf{N} dV,$$

$$\mathbf{Q}_1 = - \int_V \rho (\mathbf{A} \tilde{\omega}' \tilde{\omega}' s' + 2 \mathbf{A} \tilde{\omega}' \mathbf{N} \dot{\mathbf{p}}) dV,
 \tag{13}$$

$$\mathbf{Q}_2 = \int_V \rho \tilde{\mathbf{s}}' (\tilde{\omega}' \tilde{\omega}' s' + 2 \tilde{\omega}' \mathbf{N} \dot{\mathbf{p}}) dV,$$

$$\mathbf{Q}_3 = - \int_V \rho \mathbf{N}^T (\tilde{\omega}' \tilde{\omega}' s' + 2 \tilde{\omega}' \mathbf{N} \dot{\mathbf{p}}) dV,
 \tag{14}$$

where V represents the volume of the flexible body.

3.2 Virtual work of the elastic force

The Green–Lagrange strain tensor can be written as

$$\begin{aligned}
 \varepsilon_{ij} &= \frac{1}{2} \left[\frac{\partial u_i}{\partial x_j} + \frac{\partial u_j}{\partial x_i} + \sum_{k=1}^3 \left(\frac{\partial u_k}{\partial x_i} \right) \left(\frac{\partial u_k}{\partial x_j} \right) \right], \\
 i, j &= 1, 2, 3,
 \end{aligned}
 \tag{15}$$

where x_1, x_2 and x_3 represent the coordinates of the relative displacement vector s before deformation defined in the body-fixed frame, and u_1, u_2 and u_3 represent the coordinates of the deformation vector defined in the body-fixed frame. For $s' = [s_1 \ s_2 \ s_3]^T$, the relation between s' and $[u_1 \ u_2 \ u_3]^T$ is given by

$$[u_1 \ u_2 \ u_3]^T = [s_1 \ s_2 \ s_3]^T - [x_1 \ x_2 \ x_3]^T.
 \tag{16}$$

Substitute Eq. (16) into (15), one obtains

$$\begin{aligned}
 \varepsilon_{ij} &= \frac{1}{2} \left[\frac{\partial(s_i - x_i)}{\partial x_j} + \frac{\partial(s_j - x_j)}{\partial x_i} + \sum_{k=1}^3 \left(\frac{\partial(s_k - x_k)}{\partial x_i} \right) \right. \\
 &\quad \left. \times \left(\frac{\partial(s_k - x_k)}{\partial x_j} \right) \right], \quad i, j = 1, 2, 3,
 \end{aligned}
 \tag{17}$$

Equation (17) reads

$$\begin{aligned}
 \varepsilon_{ij} &= \frac{1}{2} \left[\sum_{k=1}^3 \left(\frac{\partial s_k}{\partial x_i} \right) \left(\frac{\partial s_k}{\partial x_j} \right) - \delta_{ij} \right] \\
 &= \frac{1}{2} \left[\left(\frac{\partial s'}{\partial x_i} \right)^T \left(\frac{\partial s'}{\partial x_j} \right) - \delta_{ij} \right] \\
 &= \frac{1}{2} \left[\mathbf{p}^T \left(\frac{\partial \mathbf{N}}{\partial x_i} \right)^T \left(\frac{\partial \mathbf{N}}{\partial x_j} \right) \mathbf{p} - \delta_{ij} \right],
 \end{aligned}
 \tag{18}$$

where

$$\delta_{ij} = \begin{cases} 1, & i = j, \\ 0, & i \neq j. \end{cases}
 \tag{19}$$

The strain tensor is given by

$$\boldsymbol{\varepsilon} = [\varepsilon_{11} \ \varepsilon_{22} \ \varepsilon_{33} \ 2\varepsilon_{12} \ 2\varepsilon_{23} \ 2\varepsilon_{31}]^T,
 \tag{20}$$

and virtual work of elastic force is written as

$$\delta W_e = - \int_V \delta \boldsymbol{\varepsilon}^T \mathbf{E} \boldsymbol{\varepsilon} dV,
 \tag{21}$$

where \mathbf{E} represents the matrix of elastic coefficients, which can be written as

$$\mathbf{E} = \begin{bmatrix} E_{11} & E_{12} & E_{13} & 0 & 0 & 0 \\ E_{21} & E_{22} & E_{23} & 0 & 0 & 0 \\ E_{31} & E_{32} & E_{33} & 0 & 0 & 0 \\ 0 & 0 & 0 & E_{44} & 0 & 0 \\ 0 & 0 & 0 & 0 & E_{55} & 0 \\ 0 & 0 & 0 & 0 & 0 & E_{66} \end{bmatrix},
 \tag{22}$$

where

$$\begin{aligned}
 E_{11} &= E_{22} = E_{33} = \lambda + 2\mu, \\
 E_{12} &= E_{21} = E_{13} = E_{31} = E_{23} = E_{32} = \lambda, \\
 E_{44} &= E_{55} = E_{66} = \mu.
 \end{aligned}
 \tag{23}$$

Substitute Eqs. (18), (20) and (22) into (21), one obtains

$$\delta W_e = -\delta \mathbf{p}^T \mathbf{K} \mathbf{p},
 \tag{24}$$

where $\mathbf{K}(\mathbf{p})$ represents the nonlinear stiffness matrix, which is given by

$$\begin{aligned} \mathbf{K} = & \frac{1}{2} \sum_{i=1}^3 \sum_{j=1}^3 \int_V E_{ij}(\mathbf{p}^T \mathbf{S}_{jj} \mathbf{p} - 1) \mathbf{S}_{ii} dV \\ & + \sum_{i=1}^3 \int_V E_{(3+i)(3+i)}(\mathbf{p}^T \mathbf{S}_{ik(i)} \mathbf{p}) [\mathbf{S}_{ik(i)} + \mathbf{S}_{k(i)i}] dV, \end{aligned} \quad (25)$$

and $k(i)$, \mathbf{S}_{ij} are defined as

$$\begin{aligned} k(i) = & \begin{cases} i+1, & i=1, 2, \\ 1, & i=3, \end{cases} \\ \mathbf{S}_{ij} = & \left(\frac{\partial \mathbf{N}}{\partial x_i} \right)^T \left(\frac{\partial \mathbf{N}}{\partial x_j} \right). \end{aligned} \quad (26)$$

Each element of the stiffness matrix is given by

$$\begin{aligned} K(\alpha, \beta) = & \frac{1}{2} \sum_{i=1}^3 \sum_{j=1}^3 \int_V E_{ij}(\mathbf{p}^T \mathbf{S}_{jj} \mathbf{p} - 1) \mathbf{S}_{ii}(\alpha, \beta) dV \\ & + \sum_{i=1}^3 \int_V E_{(3+i)(3+i)}(\mathbf{p}^T \mathbf{S}_{ik(i)} \mathbf{p}) \\ & \times [\mathbf{S}_{ik(i)}(\alpha, \beta) + \mathbf{S}_{k(i)i}(\alpha, \beta)] dV. \end{aligned} \quad (27)$$

Virtual work of elastic force can be also written as

$$\delta W_e = \delta \mathbf{q}^T \mathbf{Q}_e, \quad (28)$$

where the elastic force matrix takes the form

$$\mathbf{Q}_e = [\mathbf{0} \quad \mathbf{0} \quad -(\mathbf{K}(\mathbf{p})\mathbf{p})^T]^T. \quad (29)$$

3.3 Virtual work of body force

Let \mathbf{f} be the body force matrix defined in the inertial frame, virtual work of body force then reads

$$\delta W_f = \int_V \delta \mathbf{r}^T \mathbf{f} dV = \delta \mathbf{q}^T \mathbf{Q}_f, \quad (30)$$

where the generalized force matrix associated with the body force reads

$$\mathbf{Q}_f = \int_V [\mathbf{f}^T \quad (\tilde{\mathbf{s}}^T \mathbf{A}^T \mathbf{f})^T \quad (\mathbf{N}^T \mathbf{A}^T \mathbf{f})^T]^T dV. \quad (31)$$

3.4 Variational equations

Application of variation principle leads to the variational equations

$$\delta W_i + \delta W_e + \delta W_f = 0, \quad (32)$$

which can be written as

$$\delta \mathbf{q}^T (-\mathbf{M} \ddot{\mathbf{q}} + \mathbf{Q}) = 0, \quad (33)$$

where the generalized force matrix for B_i is given by

$$\mathbf{Q} = \mathbf{Q}_i + \mathbf{Q}_e + \mathbf{Q}_f. \quad (34)$$

4 Dynamic equations of flexible multibody systems

Variational equations of a flexible multibody system are given by

$$\sum_{i=1}^N \delta \mathbf{q}^{(i)T} (-\mathbf{M}^{(i)} \ddot{\mathbf{q}}^{(i)} + \mathbf{Q}^{(i)}) + \delta W_s = 0, \quad (35)$$

where δW_s represents virtual work of the force element.

Defining $\mathbf{q} = [\mathbf{q}^{(1)T} \dots \mathbf{q}^{(N)T}]^T$ as the global generalized coordinate vector, virtual work of the force element can be written as

$$\delta W_s = \delta \mathbf{q}^T \mathbf{Q}_s, \quad (36)$$

where \mathbf{Q}_s represents the generalized force matrix related to the force element.

For the flexible multibody system with constraint equations $\Phi(\mathbf{q}, t) = \mathbf{0}$, Lagrange's equations of the first kind with Lagrange multipliers and the acceleration equations read

$$\begin{bmatrix} \mathbf{M}_g & \Phi_q^T \\ \Phi_q & \mathbf{0} \end{bmatrix} \begin{bmatrix} \ddot{\mathbf{q}} \\ \lambda \end{bmatrix} = \begin{bmatrix} \mathbf{Q}_g \\ -(\Phi_q \dot{\mathbf{q}})_q \dot{\mathbf{q}} - 2\Phi_{qt} \dot{\mathbf{q}} - \Phi_{tt} \end{bmatrix}, \quad (37)$$

where Φ_q represents the Jacobian matrices, and λ represents the Lagrange multipliers related to the corresponding constraint equations, and \mathbf{M}_g , \mathbf{Q}_g represent the system generalized mass and force matrices of the flexible multibody system, which are given by

$$\begin{aligned} \mathbf{M}_g = & \text{diag}(\mathbf{M}^{(1)}, \dots, \mathbf{M}^{(N)}), \\ \mathbf{Q}_g = & \mathbf{Q}_s + [\mathbf{Q}^{(1)T}, \dots, \mathbf{Q}^{(N)T}]^T. \end{aligned} \quad (38)$$

5 Matrix separation method for stiffness matrix

In order to calculate each element of the stiffness matrix efficiently, Eq. (27) can be rewritten as

$$K(\alpha, \beta) = \mathbf{p}^T \mathbf{C}_{\alpha\beta} \mathbf{p} + c_{\alpha\beta}, \quad (39)$$

where

$$C_{\alpha\beta} = \frac{1}{2} \sum_{i=1}^3 \sum_{j=1}^3 \int_V E_{ij} S_{ii}(\alpha, \beta) S_{jj} dV + \sum_{i=1}^3 \int_V E_{(3+i)(3+i)} [S_{ik(i)}(\alpha, \beta) + S_{k(i)i}(\alpha, \beta)] \times S_{ik(i)} dV, \tag{40}$$

$$c_{\alpha\beta} = -\frac{1}{2} \sum_{i=1}^3 \sum_{j=1}^3 \int_V E_{ij} S_{ii}(\alpha, \beta) dV. \tag{41}$$

It can be seen that by separating coordinate matrix $\mathbf{p}(t)$ from the integration matrix, the constant matrix $C_{\alpha\beta}$ for each element of the stiffness matrix can be calculated before time integration begins, such that only matrix multiplication is needed for each time step and computational efficiency can be improved.

6 Comparison of different models

6.1 Linear model

In a linear model, the displacement of an arbitrary point on the beam is written as

$$u_1 = u_{10} - x_2 \frac{\partial u_2}{\partial x_1} - x_3 \frac{\partial u_3}{\partial x_1}, \tag{42}$$

where u_{10} represents the longitudinal deformation of the corresponding point on the neutral axis, and the relation between strain and deformation displacement is given by

$$\varepsilon_{11} \approx \frac{\partial u_1}{\partial x_1}. \tag{43}$$

In such model, the quadratic term of the strain is ignored, which is closely related to the stiffening terms in dynamic equations. Therefore, linear model fails to explain the stiffening effect due to the high rotating speed.

6.2 Low-order approximate nonlinear model

In order to include the stiffening terms in the equations of motion, a low-order approximate nonlinear model is used. In such a model, a non-Cartesian variable w is led into the expression of the longitudinal deformation [4]

$$u_1 = w - \frac{1}{2} \int_0^{x_1} \left[\left(\frac{\partial u_2}{\partial \xi} \right)^2 + \left(\frac{\partial u_3}{\partial \xi} \right)^2 \right] d\xi - x_2 \frac{\partial u_2}{\partial x_1} - x_3 \frac{\partial u_3}{\partial x_1}, \tag{44}$$

and the axial strain is given by

$$\varepsilon_{11} \approx \frac{\partial u_1}{\partial x_1} + \frac{1}{2} \left[\left(\frac{\partial u_2}{\partial x_1} \right)^2 + \left(\frac{\partial u_3}{\partial x_1} \right)^2 \right] = \frac{\partial w}{\partial x_1} - x_2 \frac{\partial^2 u_2}{\partial x_1^2} - x_3 \frac{\partial^2 u_3}{\partial x_1^2}. \tag{45}$$

Equation 44 shows that the use of variable w may produce high-order deformation terms in the mass and inertia force matrices. However, with the assumption of small deformation, the mass and force matrices are approximated to the second order. For each element of \mathbf{M} and \mathbf{Q} , one obtains

$$M_{ij}(\mathbf{p}) \approx M_{ij}^0 + M_{ij}^1 \mathbf{p} + \mathbf{p}^T M_{ij}^2 \mathbf{p}, \tag{46}$$

$$Q_i(\mathbf{p}, \dot{\mathbf{p}}) \approx Q_i^0 + Q_i^1 \mathbf{p} + Q_i^2 \dot{\mathbf{p}} + \mathbf{p}^T Q_i^3 \mathbf{p} + \mathbf{p}^T Q_i^4 \dot{\mathbf{p}} + \dot{\mathbf{p}}^T Q_i^5 \dot{\mathbf{p}}.$$

Because in a low-order approximate nonlinear model, the high-order deformation terms are not taken into account, such formulation is only suitable for simulation of flexible multibody systems with small deformation.

6.3 Present nonlinear model

In the present formulation, the axial strain is given in an exact form

$$\varepsilon_{11} = \frac{\partial u_1}{\partial x_1} + \frac{1}{2} \left[\left(\frac{\partial u_1}{\partial x_1} \right)^2 + \left(\frac{\partial u_2}{\partial x_1} \right)^2 + \left(\frac{\partial u_3}{\partial x_1} \right)^2 \right], \tag{47}$$

and employing the relative Cartesian coordinates and slopes defined in the body-fixed frame instead of the deformation coordinates, the mass and force matrices are simplified and accurate without the need to consider high-order deformation terms.

7 Simulation examples

7.1 Accuracy and efficiency verification

A flexible single pendulum is shown in Fig. 2. The geometric property and material data of each beam are: mass density $\rho = 5,540 \text{ kg/m}^3$, the modulus of elasticity $E = 7 \times 10^5 \text{ N/m}^2$, length $l = 1.2 \text{ m}$, area $A = 0.0018 \text{ m}^2$, moment of inertia $I = 1.215 \times 10^{-8} \text{ m}^4$. Initially, the beam is in horizontal and static state without deformation, and then applied with gravitational force, the flexible single pendulum undergoes a periodic motion. The beam is divided into four elements, and Gear integration method is employed for the numerical simulation. The time step is 10^{-4} s , and the error tolerance is 10^{-8} m .

The displacement of the tip point in i_0 and j_0 directions are shown in Figs. 3 and 4. Agreement of the present results with

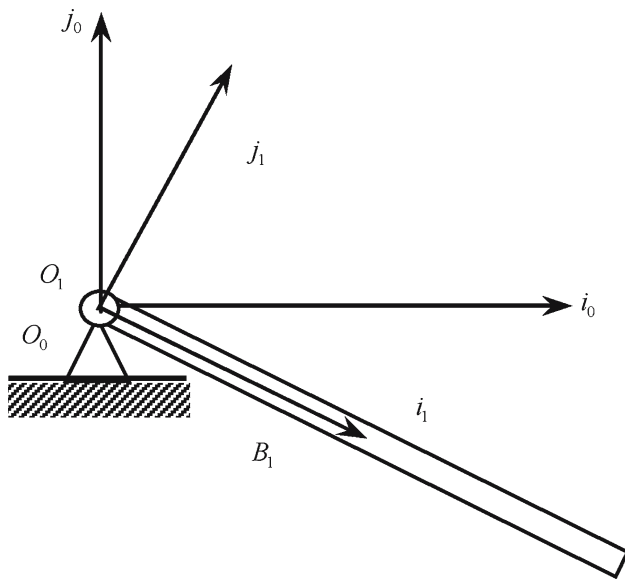


Fig. 2 Flexible single pendulum

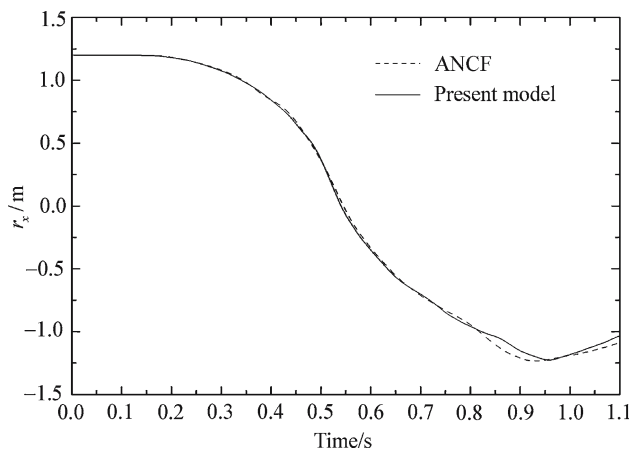


Fig. 3 Tip displacement component in x direction

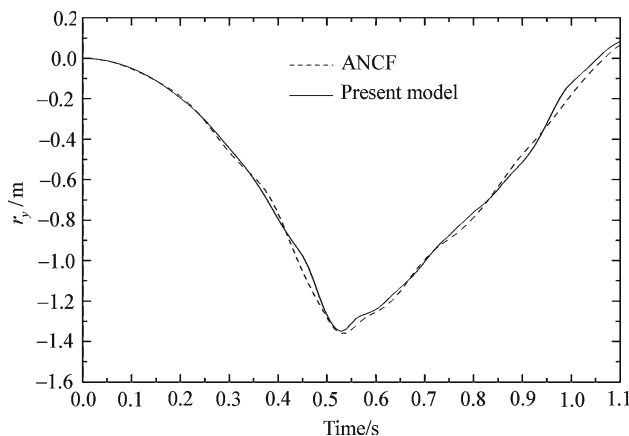


Fig. 4 Tip displacement component in y direction

Table 1 Efficiency of the matrix separation method

	With matrix separation (s)	Without matrix separation (s)
Consumed time	30	300

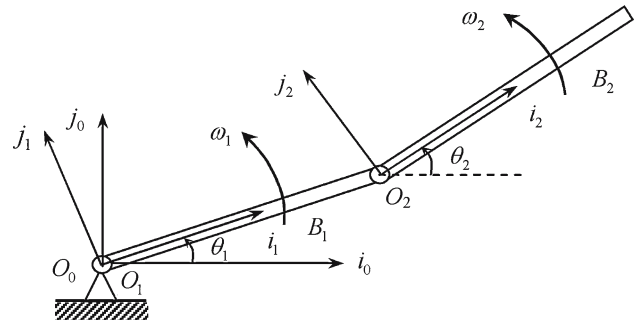


Fig. 5 Two flexible beams

those obtained by the absolute nodal coordinate formulation (ANCF) verifies the correctness of the present formulation for the dynamic analysis.

Efficiency of the proposed matrix separation method can be verified by comparison of the consumed time for the present formulation and the previous formulation without matrix separation. Table 1 shows that the consumed time of the present formulation is 10% of the formulation without matrix separation.

7.2 Geometric stiffening effect

Two flexible beams are shown in Fig. 5. Beam B_2 is connected to B_1 , and B_1 is connected to the ground with revolute joints. The geometric property and material data of each beam are: mass density $\rho = 2.7667 \times 10^3 \text{ kg/m}^3$, the modulus of elasticity $E = 6.8952 \times 10^{10} \text{ N/m}^2$, length $l = 4 \text{ m}$, area $A = 4 \times 10^{-4} \text{ m}^2$, moment of inertia $I = 1.33 \times 10^{-8} \text{ m}^4$. In this simulation, body force is not taken into account.

Initially, the body fixed frames of the two beams are parallel to the inertial frame without deformation, thus, $\mathbf{r}_0^{(1)}(0) = \mathbf{0}$, $\mathbf{r}_0^{(1)}(0) = [l \ 0]^T$, $\theta_1(0) = 0$, $\theta_2(0) = 0$, $\mathbf{p}_1(0) = \mathbf{0}$, $\mathbf{p}_2(0) = \mathbf{0}$. The initial angular velocities for B_1 and B_2 are $\dot{\theta}_1(0) = 4 \text{ rad/s}$ and $\dot{\theta}_2(0) = 4 \text{ rad/s}$, respectively.

The time history of the tip transverse deformation of B_1 is shown in Figs. 6 and 7. It can be seen that in case of high rotating speed, the deformation results obtained by the linear model are quite different from those obtained by the two nonlinear models. The large amplitude and low frequency vibration of the tip transverse deformation show the characteristics of the softening effect of such model, such that the linear model cannot be used for the dynamic analysis of the stiffening problem. The agreement of the results of

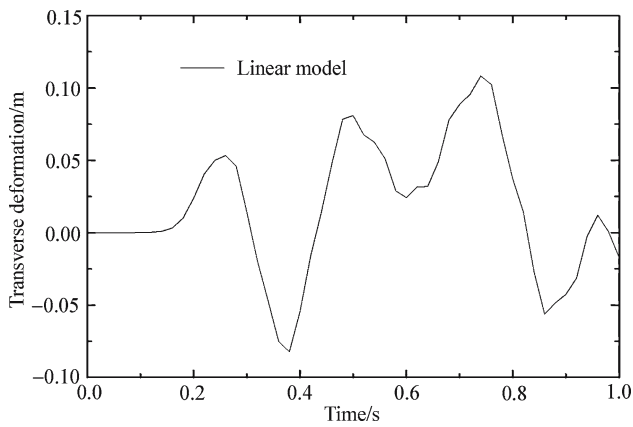


Fig. 6 Tip transverse deformation of B_2

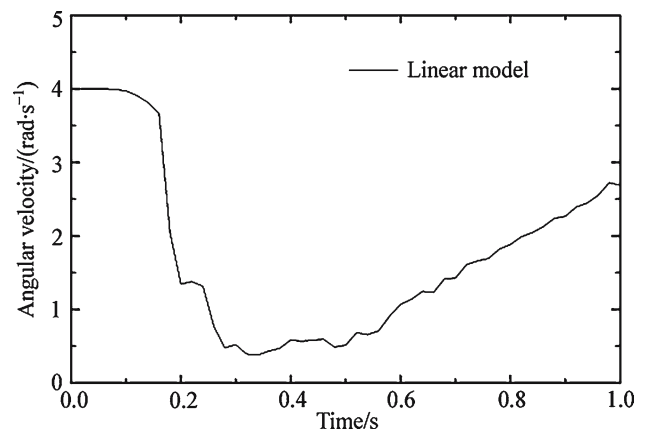


Fig. 8 Angular velocity of B_1

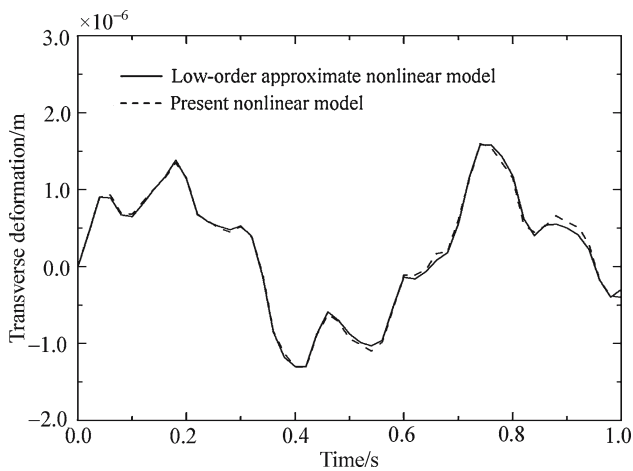


Fig. 7 Tip transverse deformation of B_2

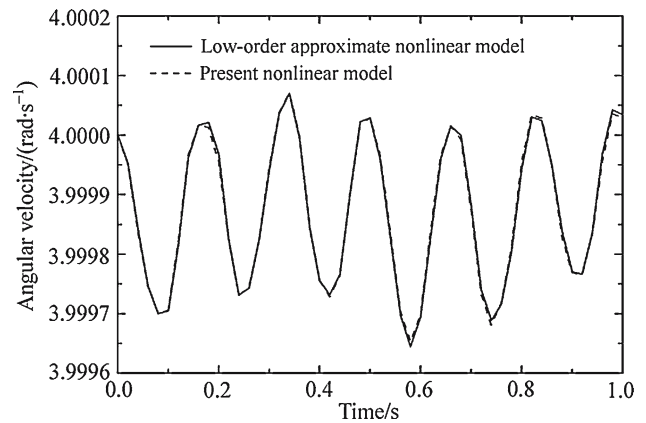


Fig. 9 Angular velocity of B_1

the low-order approximate nonlinear model and the present model verifies the effectiveness of the low-order approximate nonlinear model for the stiffening analysis of a multibody system with high rotating speed and small deformation. Figures 8 and 9 show that due to the coupling of deformation and rotational motion, the angular velocity of B_1 obtained by the linear model is also different from those obtained by the nonlinear models.

7.3 Large deformation effect

The influence of large deformation on dynamic performance of a hub-beams system is shown in the following section. As shown in Fig. 10, the hub is connected with a rotational spring, and B_1 is connected to the hub with a fixed joint. The stiffness of the rotational spring is 1,000Nm/rad. The radius and rotary inertia of the hub are 0.5 m and 10 kg m², respectively. Each beam has the same geometric and material properties as the example in Sect. 7.1.

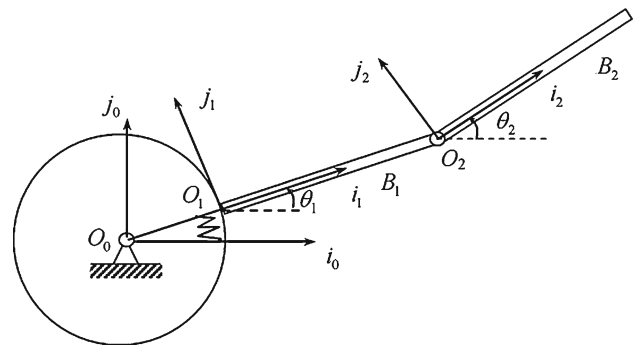


Fig. 10 Hub-beams system with rotational spring

Initially, the beams are in static state without deformation, $\theta_1(0) = \theta_0 = 0.15$ rad, $\theta_2(0) = 0$, thus,

$$\begin{aligned} \mathbf{r}_0^{(1)} &= [R \cos \theta_0 \quad R \sin \theta_0], \\ \mathbf{r}_0^{(2)} &= [(R + l) \cos \theta_0 \quad (R + l) \sin \theta_0], \\ \mathbf{p}_1(0) &= \mathbf{0}, \quad \mathbf{p}_2(0) = \mathbf{0}. \end{aligned}$$

The time histories of the tip transverse deformation and rotational angle of B_1 are shown in Figs. 11 and 12. It can be seen that due to the excitation of the high-frequency spring

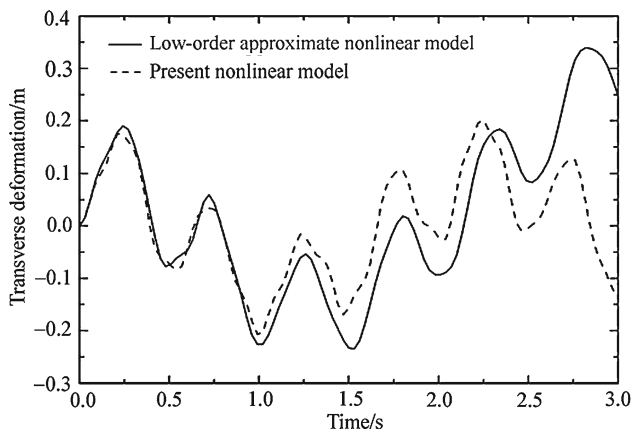


Fig. 11 Tip transverse deformation of B_1

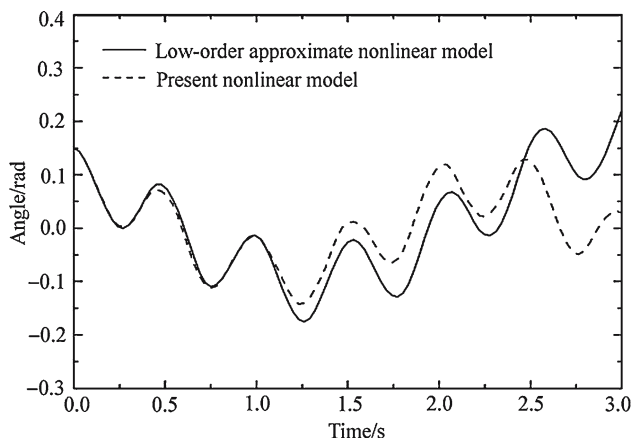


Fig. 12 Rotational angle of B_1

torque, the deformation is large enough (approximate 5% of the beam length) to cause simulation errors in case that the low-order approximate formulation is used, since the high order deformation terms are not included in the mass and force matrices in such model. It is shown that the amplitude of vibration of the tip transverse deformation and rotational angle obtained by the low-order model gradually increases, which may lead to divergence of the deformation results. However, it can be seen that the vibration of the deformation and rotational angle obtained by the present model is stable, which verifies the effectiveness of the present model for the dynamic analysis of a flexible multibody system with large deformation.

8 Conclusions

A new hybrid-coordinate formulation considering the geometric nonlinear effect is proposed. On the basis of the exact strain–displacement relation, such formulation is

suitable for simulation of a flexible multibody system with large deformation. Agreement of the present results with those obtained by the ANCF verifies the correctness of the proposed formulation. Comparison of the present results with those obtained by the linear model and low-order approximate nonlinear model shows that the linear model fails to explain the stiffening problem due to the neglect of the quadratic terms in the strain–displacement relationship. In addition, it is shown that the low-order approximate nonlinear model succeeds in explaining the dynamic stiffening phenomenon. However, due to the neglect of the high-order deformation terms in the mass and force matrices, such method is not suitable for the simulation of the flexible multibody system with large deformation.

References

1. Kane, T.R., Ryan, R.R., Banerjee, A.K.: Dynamics of a cantilever beam attached to a moving base. *J. Guid. Control Dyn.* **10**, 139–150 (1987)
2. Wallrapp, O., Schwertassek, R.: Representation of geometric stiffening in multibody system simulation. *Int. J. Numer. Methods Eng.* **32**, 1833–1850 (1991)
3. Ryu, J., Kim, S.S.: A general approach to stress stiffening effects on flexible multibody dynamic systems. *Mech. Struct. Mach.* **22**, 157–180 (1994)
4. Liu, J.Y., Hong, J.Z.: Study on modeling theory of rigid-flexible coupling dynamic system (in Chinese). *Acta Mech. Sin.* **34**(3), 408–415 (2002)
5. Liu, J.Y., Hong, J.Z.: Geometric stiffening effect on rigid-flexible coupling dynamics of an elastic beam. *J. Sound Vib.* **278**, 1147–1162 (2004)
6. Yang, H.: Study on dynamic modeling theory and experiments for rigid-flexible coupling systems (in Chinese). Ph.D. dissertation. Shanghai Jiao Tong University (2002)
7. Escalona, J.L., Hussien, H.A., Shabana, A.A.: Application of the absolute nodal co-ordinate formulation to multibody system dynamics. *J. Sound Vib.* **214**, 883–851 (1998)
8. Berneri, M., Shabana, A.A.: Development of simple models for the elastic forces in the absolute nodal coordinate formulation. *J. Sound Vib.* **235**, 539–565 (2000)
9. Omar, M.A., Shabana, A.A.: A two-dimensional shear deformable beam for large rotation and deformation problems. *J. Sound Vib.* **243**, 565–576 (2001)
10. Dombrowski, S.V.: Analysis of large flexible body deformation in multibody systems using absolute coordinates. *Multibody Syst. Dyn.* **8**, 409–432 (2002)
11. Dmitrochenko, O.N., Pogorelov, D.Y.: Generalization of plate finite elements for absolute nodal coordinate formulation. *Multibody Syst. Dyn.* **10**, 17–43 (2003)
12. Liu, J.Y., Hong, J.Z.: Nonlinear formulation for flexible multibody system with large deformation. *Acta Mech. Sin.* **23**(1), 111–119 (2007)